EurJIC
European Journal of Inorganic Chemistry

Research Article
doi.org/10.1002/ejic.202500245

Chemistry Europe
European Chemical Societies Publishing

www.eurjic.org

A Bis-Thiosemicarbazone Pd(II) SiO_2 Nanoparticle Conjugate for C—C Coupling Catalysis

Eric Tobechukwu Anthony, Selina Olthof, Stefan Roitsch, Klaus Meerholz, Sanjay Mathur, and Axel Klein*

Pd(II) complexes of thiosemicarbazones (TSCs) have previously been used as homogenous precatalysts for constructing C—C bonds. Herein, the first SiO_2-supported homogeneous Pd(II)-TSC catalyst [PdL]–APTES–SiO_2 (APTES = (3-aminopropyl)triethoxysilane) is reported for this purpose. This Pd complex–SiO_2 nanoparticle (NP) conjugate is synthesized through covalent binding of the pentadentate bis(*N*4-(2-ethylphenyl)) 2,6-diacetyl-pyridine TSC onto monodispersed SiO_2, followed by coordination of Pd(II). Characteristic shifts of resonances in the Fourier-transform infrared spectra allowed confirming the SiO_2 functionalization and the Pd-binding. High-resolution X-ray photoelectron spectroscopy (XPS) analysis of N 1*s*, C 1*s*, and S 2*p* shows that the binding energies of the atoms in the C═N, C═S, C—N, N—H, pyridine-N, and imine-N groups shift to lower values upon Pd coordination. The absence of chloride in the XPS of the H_2L–APTES–SiO_2 conjugate strongly supports the successful covalent binding of the TSC onto the SiO_2 NPs and is in line with the $S_{thiolate}$^N_{imine}^$N_{pyridine}$^N_{amide} coordination of Pd(II) in the conjugate that is also found in the model complex [Pd(L)]. The [PdL]–APTES–SiO_2 NPs are used as precatalyst in Suzuki–Miyaura-type cross-coupling reactions with yields ranging from 70% to 83%.

1. Introduction

The Pd-catalyzed Suzuki–Miyaura cross-coupling reaction that uses organoboron and organohalide precursors is a powerful method to construct C(sp^2)—C(sp^2) bonds.[1–4] Pd (pre)catalysts such as $Pd(OAc)_2$, [Pd_2(dba)$_3$] (dba = dibenzylideneacetone), and [$Pd(PPh_3)_4$] combined with suitable ligands represent typical homogenous catalytic systems.[1–6] Homogenous catalytic system generally show higher chemo and regioselectivity.[1,2,4,6] However, the separation of the catalysts from the reaction products is difficult and hampers an industrial-scale use of this method.[4,6,7] Heterogeneous Suzuki–Miyaura catalysts such as so-called ligand-free Pd catalysts,[4,8,9] 3D-printed Pd complexes,[10] or Pd nanoparticle (NP)-based systems,[4,11,12] can be easily separated, but show reduced efficiency in terms of reactivity per Pd atom and low regioselectivity.[11–13] The combination of both approaches, homogeneous Pd catalysts (complexes) that are covalently anchored on a solid support,[12–20] allows easy separation, recycling, and reuse of the catalyst, while the Pd reaction center is identical to a homogeneous catalyst center and the same reactivity and selectivity can be expected.[12,16,20] For the anchoring on a Pd complex onto an NP support, the ligand must offer the opportunity of simple modification to allow the covalent bonding (conjugation) without changing the binding properties of the ligand.

Thiosemicarbazones (TSCs) are a class of remarkable ligands featuring soft thione or thiol(ate) S atoms for coordination, along with several soft imine or amine N atoms (**Scheme 1**A and B). What makes them especially attractive as ligands for NP-supported Pd catalysts is their modular synthesis from carbonyls and thiosemicarbazides allowing to introduce up to four different substituents R (Scheme 1A).[21–28] and the possibility of extending the primary N^S donor set, creating polydentate TSC ligands (Scheme 1B).[21–28] The thione–thiol tautomerism (Scheme 1A) contributes further to the design of such polydentate TSC ligands as it can help to balance the charge of the coordinated metal ion with either a neutral thione or an anionic thiolate (Scheme 1B).[21,26,28–30]

In a very recent study, Pd(II) complexes containing tridentate TSC ligands with a remarkable structural wealth, were used for Pd-catalyzed Suzuki–Miyaura cross-coupling reactions (Scheme 1C).[31] Nevertheless, the number of Pd(II) TSC complexes used in Suzuki–Miyaura cross-coupling or related C—C cross-coupling reactions remained relatively small so far.[21,24,25,31–42]

TSC Pd(II) complexes covalently anchored on solid supports as catalysts in the Suzuki–Miyaura cross-coupling reactions were not yet reported, while the covalent anchoring of TSC ligands on various supports for other purposes has previously been reported.[28] C-based polymers like chitosan or cellulose have been functionalized with thiophenes for Cu(II) binding.[43,44]

E. Tobechukwu Anthony, S. Mathur, A. Klein
University of Cologne
Faculty of Mathematics and Natural Sciences
Department of Chemistry and Biochemistry
Institute for Inorganic and Materials Chemistry
Greinstrasse 6, D–50939 Cologne, Germany
E-mail: axel.klein@uni-koeln.de

S. Olthof, S. Roitsch, K. Meerholz
University of Cologne
Faculty of Mathematics and Natural Sciences
Department of Chemistry and Biochemistry
Institute for Light and Matter
Greinstrasse 4-6, D–50939 Cologne, Germany

Supporting information for this article is available on the WWW under https://doi.org/10.1002/ejic.202500245

Research Article
doi.org/10.1002/ejic.202500245

Chemistry Europe
European Chemical Societies Publishing

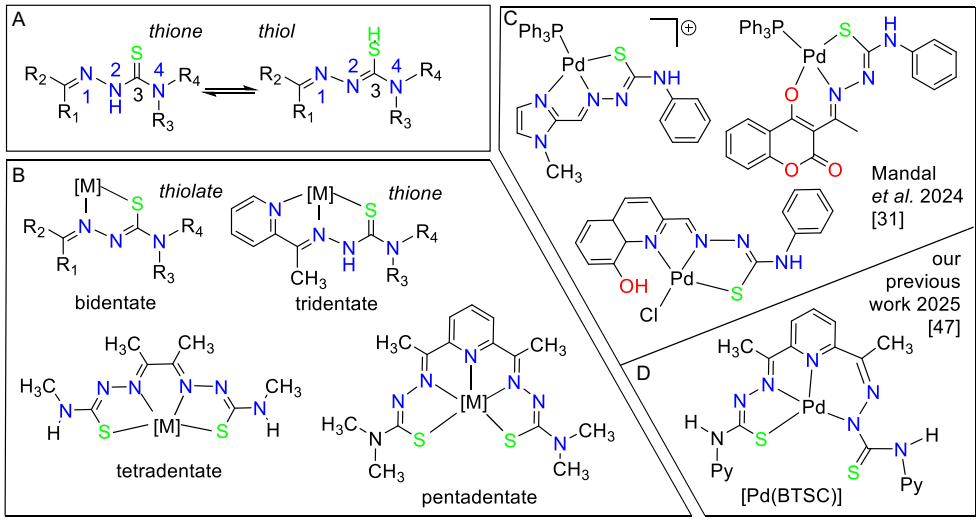

Scheme 1. A) General formula and thione and thiol tautomers in TSCs. B) Metal complexes with bi- and tridentate TSC ligands and tetra- and pentadentate bis-TSC ligands. C) Previously reported Pd(II) TSC complexes for D) Suzuki–Miyaura-type reactions. Adopted from ref. [31]. A previously reported Pd(II) complex with a bis-TSC ligand. Adopted from ref. [47].

Multiwalled carbon nanotubes (MWCNs) were modified with isatin TSC for Pb(II) removal[45] and SiO_2–isatin TSC conjugates were used for potentiometric monitoring of Cu(II) ions.[46] We have very recently contributed to this topic by covalently linking the pentadentate 2,6-diacetylpyridine-bis-(4-*N*-2-pyridyl)-TSC (BTSC) through APTES (APTES = (3-aminopropyl)triethoxysilane) to Fe_3O_4–SiO_2 core–shell NPs.[47] The Fe_3O_4@SiO_2–APTES–BTSC conjugate was used for Pd(II) binding from aqueous solutions, while the formation of Pd(II) complexes with such potentially pentadentate S^N^N'^N^S TSC ligands was studied on the model complex [Pd(BTSC)] (Scheme 1D) experimentally and through density functional theory (DFT) calculations.[47]

In this study, three very similar pentadentate 2,6-diacetylpyridine-bis-(4-*N*-2-pyridyl) TSCs, a TSC–APTES–SiO_2 conjugate and its corresponding Pd(II) complex were synthesized (**Scheme 2**). H_2L is a typical pyridine-1,3-carboxaldehyde-based bis-TSC. The Cl derivative H_2L–Cl bears a chloro functional group at the 4 position of the central pyridine moiety for covalent functionalization. Silica (SiO_2) NPs are attractive as support because of its chemical and mechanical stability, optical transparency, and biocompatibility.[48,49] The pentadentate TSC was covalently bound to SiO_2 NPs through APTES and the corresponding TSC–APTES–SiO_2 conjugate was coordinated to Pd(II) to form the [PdL]–APTES–SiO_2 conjugate. By a combination of

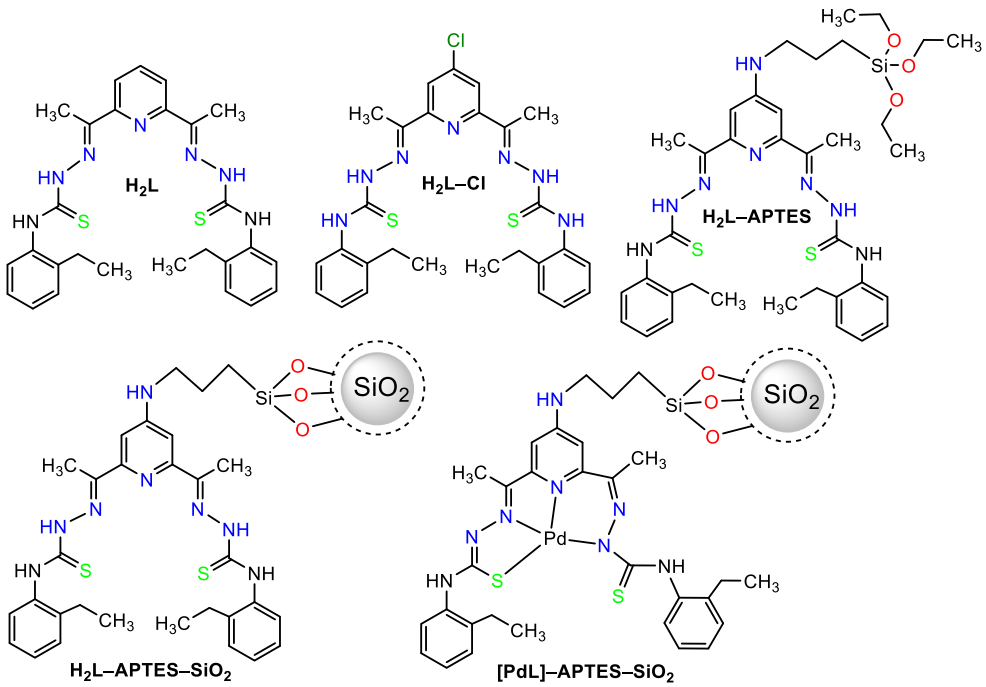

Scheme 2. Schematic drawings of the TSCs H_2L, H_2L–Cl, and H_2L–APTES, and the H_2L–APTES–SiO_2 and [PdL]–APTES–SiO_2 conjugate studied in this work.

Research Article
doi.org/10.1002/ejic.202500245

Fourier-transform infrared (FT-IR) spectroscopy, UV–vis absorption spectroscopy, and especially X-ray photoelectron spectroscopy (XPS), we were able to monitor the generation of the [PdL]–APTES–SiO_2 conjugate step-by-step. This conjugate represents the first NP-supported homogeneous TSC-based Pd(II) precatalyst and was used in Suzuki–Miyaura type of C—C cross-coupling catalysis.

2. Results and Discussion

2.1. Syntheses and Characterization of the Materials

The TSC H_2L and its 4-chloro derivative H_2L–Cl were obtained from 4-(2-ethylphenyl)-thiosemicarbazide and 2,6-diacetyl-pyridine or 4-chloro-2,6-diacetyl-pyridine in 49% and 29% yield, respectively. H_2L–Cl was reacted with APTES to obtain H_2L–APTES in 63% yield. In parallel, H_2L was reacted with K_2PdCl_4 to produce the model complex [Pd(L)] in 75% yield (**Scheme 3**, details in the Experimental Section).

Single-crystal X-ray diffraction of the model complex [Pd(L)] (data in Table S1 and S2) showed a tetradentate coordination through $S_{thiolate}$^$N1_{imine}$^$N_{Pyridine}$^$N2'_{amide}$ (Scheme 3), leaving one uncoordinated thione (C═S) group (Figure S12–S15), exactly what has been found for the previously reported [Pd(BTSC)] complex containing 2-pyridyl at the TSC N4 position instead of 2-ethyl-benzene (Scheme 1D).[47] DFT-calculated metrics and the FT-IR spectrum of [Pd(L)] (Figure S16) agreed quite well with the experimental data (Table S2).

We then prepared monodispersed APTES–SiO_2 NPs with a mean diameter of 207 nm as determined by transmission electron microscopy (TEM; Figure S17). They were reacted with H_2L–Cl to yield the H_2L–APTES–SiO_2 conjugate NPs, which were coordinated with Pd(II), generating the [PdL]–APTES–SiO_2 NPs (**Scheme 4**). The formation of the Pd-coordinated material was monitored through UV–vis absorption (Figure S22), and FT-IR spectroscopy (see later).

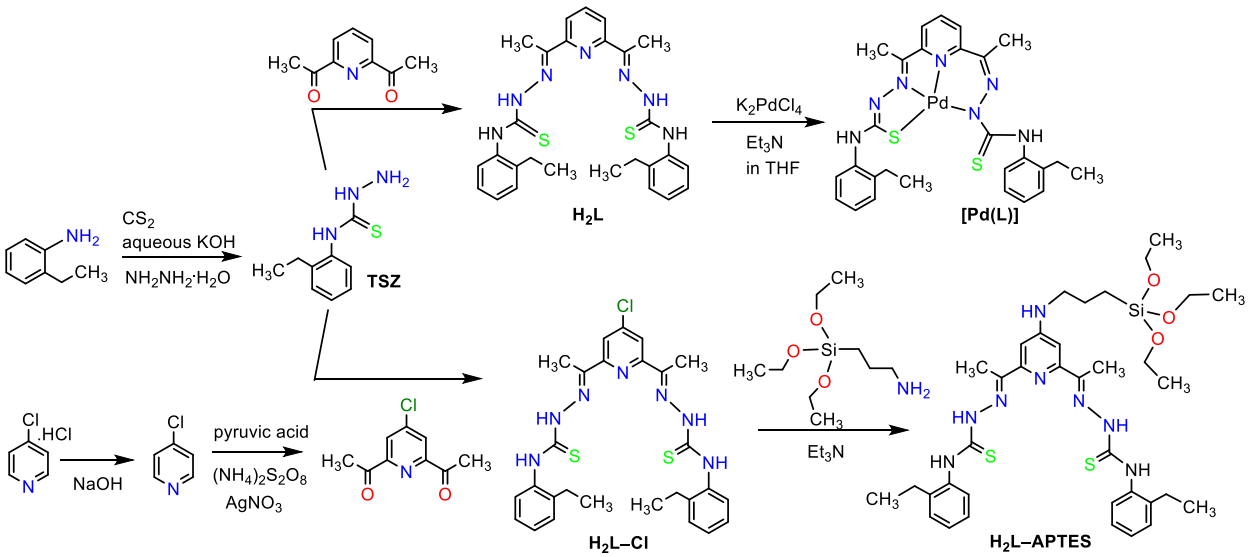

Scheme 3. Synthesis of H_2L, H_2L–Cl, H_2L–APTES, and [Pd(L)].

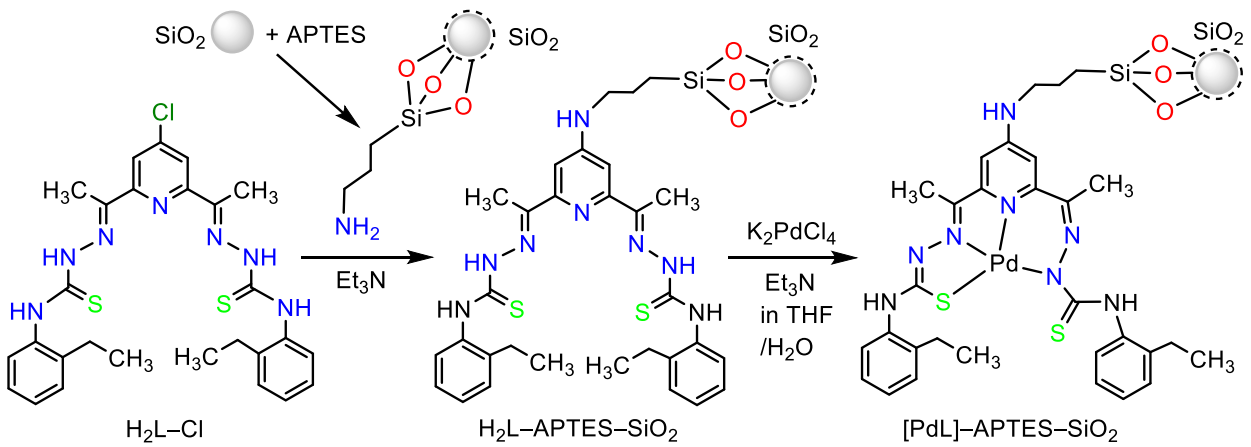

Scheme 4. Synthesis of H_2L–APTES–SiO_2 and [PdL]–APTES–SiO_2 NPs.

Research Article
doi.org/10.1002/ejic.202500245

2.2. Thermal Analysis and Powder X-Ray Diffraction

The thermogravimetric analysis (TGA) shows weight loss of about 10%, 15%, and 28% for SiO_2, APTES–SiO_2, and H_2L–APTES–SiO_2, respectively (Figure S18). The initial weight loss of about 10% for all samples at temperatures between 30 and 300 °C is attributed to adsorbed solvents. The additional 5% and 13% between 400 and 800 °C are attributed to the decomposition of APTES and H_2L.

The powder X-ray diffraction patterns of all materials appeared amorphous (Figure S18), with a single broad peak at 2θ slightly above 20°, indicative for spherical SiO_2 NP from a Stöber-type preparation ($2\theta = 21.18°$).[50–52] The noncrystalline nature of the particles is preserved after functionalizing with APTES and covalently bonding with the TSC ligand.[46]

2.3. FT-IR Spectroscopy

The spectrum of H_2L–Cl shows intense peaks at 748 and 864 cm^{-1} (**Figure 1**B), corresponding to C—Cl and C═S vibrations, and strong bands between 1515 and 1588 cm^{-1} (Figure 1A) corresponding to C═N stretching, based on comparison with 9-undecenal-TSC.[53] The bands at 2956 and 3330 cm^{-1} are assigned to asymmetrical N—H stretching, based on comparison with coumarin–TSC and benzaldehyde–TSC conjugates.[54,55] On the pristine SiO_2, the intense bands at 450 and 1076 cm^{-1} correspond to the bending and stretching of Si—OH and the asymmetric stretching of the Si—O—Si bond, respectively.[47–49] When coating SiO_2 with APTES, two additional bands appeared at 1863 and 2982 cm^{-1} corresponding to C—H and N—H vibrations alongside the Si—O deformation band at 1634 cm^{-1}. Additional bands were observed at 1494, 1561, and 2885 cm^{-1} on covalent functionalization with H_2L–Cl (Figure 1C and D). The bands were assigned to N—H bending, C═S vibration and N—H stretching, from comparison with ethyl-pyrrole–TSC.[56] New bands were observed after the coordination of Pd(II) at 668 and 1384 cm^{-1} (Figure 1B and D) assigned to Pd–N and Pd–S stretchings.[57]

2.4. XPS

The main peaks observed in the survey scan for H_2L–APTES–SiO_2 NPs are Si 2*p*, Si 2*s*, Cl 2*p*, C 1*s*, N 1*s*, and O 1*s* centered around 103, 153, 285, 400, and 532 eV (**Figure 2**). For the survey scan of

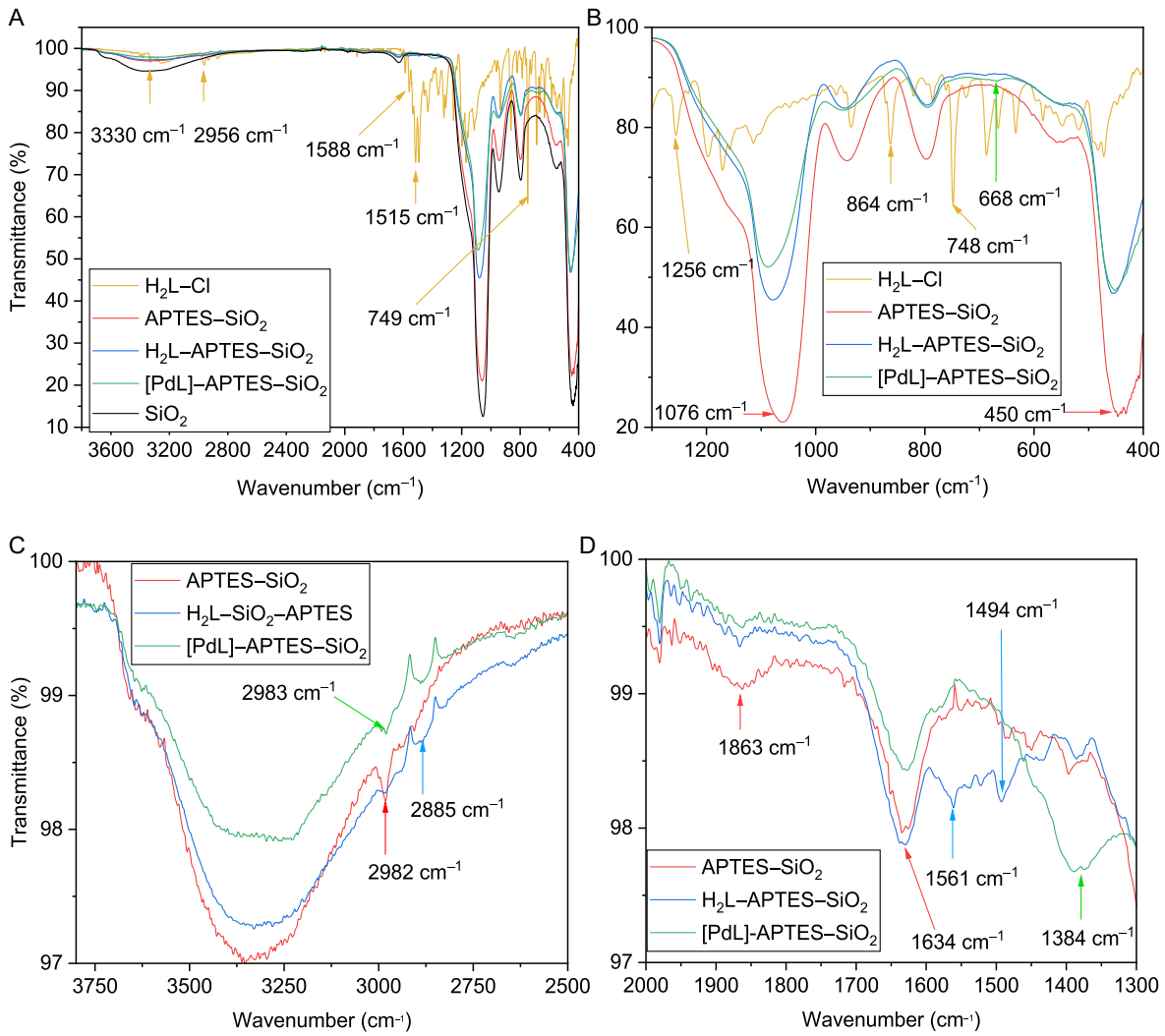

Figure 1. FT-IR spectra of H_2L–Cl, SiO_2, APTES–SiO_2, H_2L–APTES–SiO_2, and [PdL]–APTES–SiO_2.

Research Article
doi.org/10.1002/ejic.202500245

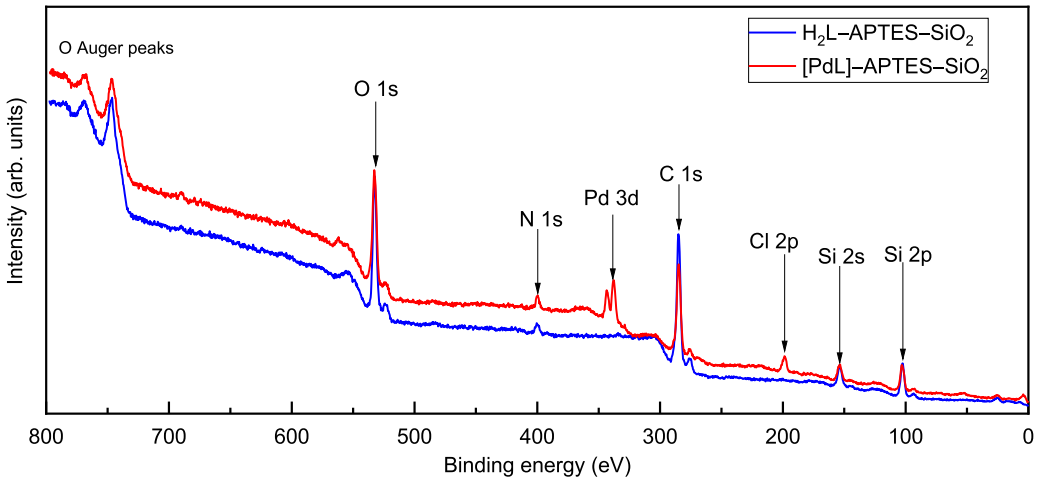

Figure 2. XPS survey scans for H_2L–APTES–SiO_2 and [PdL]–APTES–SiO_2 NPs.

[PdL]–APTES–SiO_2 NPs, additional peaks appeared for Cl 2*p* and Pd 3*d* centered around 198 and 338 eV, respectively (**Figure 3**). The absence of Cl 2*p* in the survey scan of H_2L–APTES–SiO_2 is a strong indication that the covalent anchoring of H_2L to the SiO_2 NPs was successful.

The high-resolution XPS C 1s spectrum of H_2L–APTES–SiO_2 can be deconvoluted into three peaks: C—C (284.5 eV), C—N (286.2 eV), and C═N (288.3 eV) (Figure 3).[58,59] On coordination with Pd(II), C—N (285.9 eV) and C═N (287.9 eV) shifted to a lower binding energies, in line with the C═N binding to the metal (**Figure 4**).[60] In contrast to this, the binding energy of C—C (284.6 eV) remains unchanged as the C—C group is not involved in metal-binding. The N 1*s* spectra are deconvoluted into two peaks: pyridine N (401.1 eV) and amine N (399.6 eV).[61] After

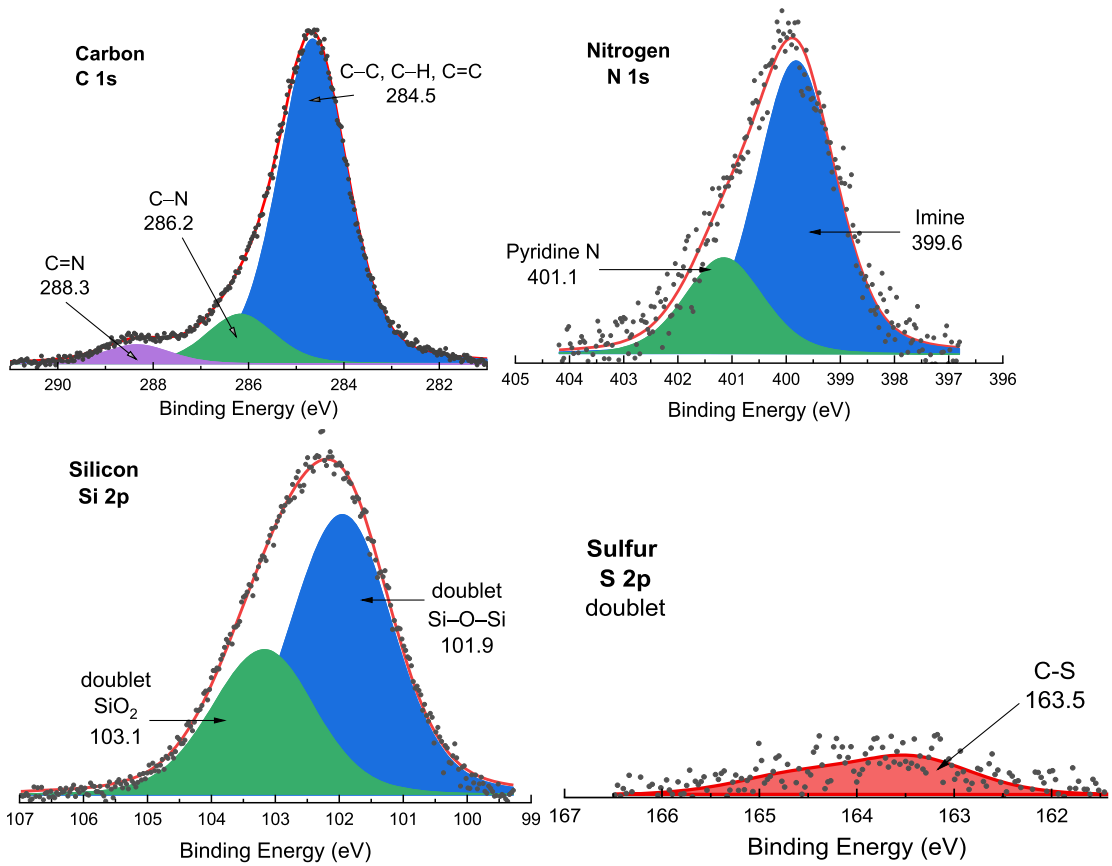

Figure 3. XPS high-resolution spectra of H_2L–APTES–SiO_2 NPs. The measured datapoints are shown, the fitted individual peak contributions are highlighted in color while the total fit is given by the red solid line.

Research Article
doi.org/10.1002/ejic.202500245

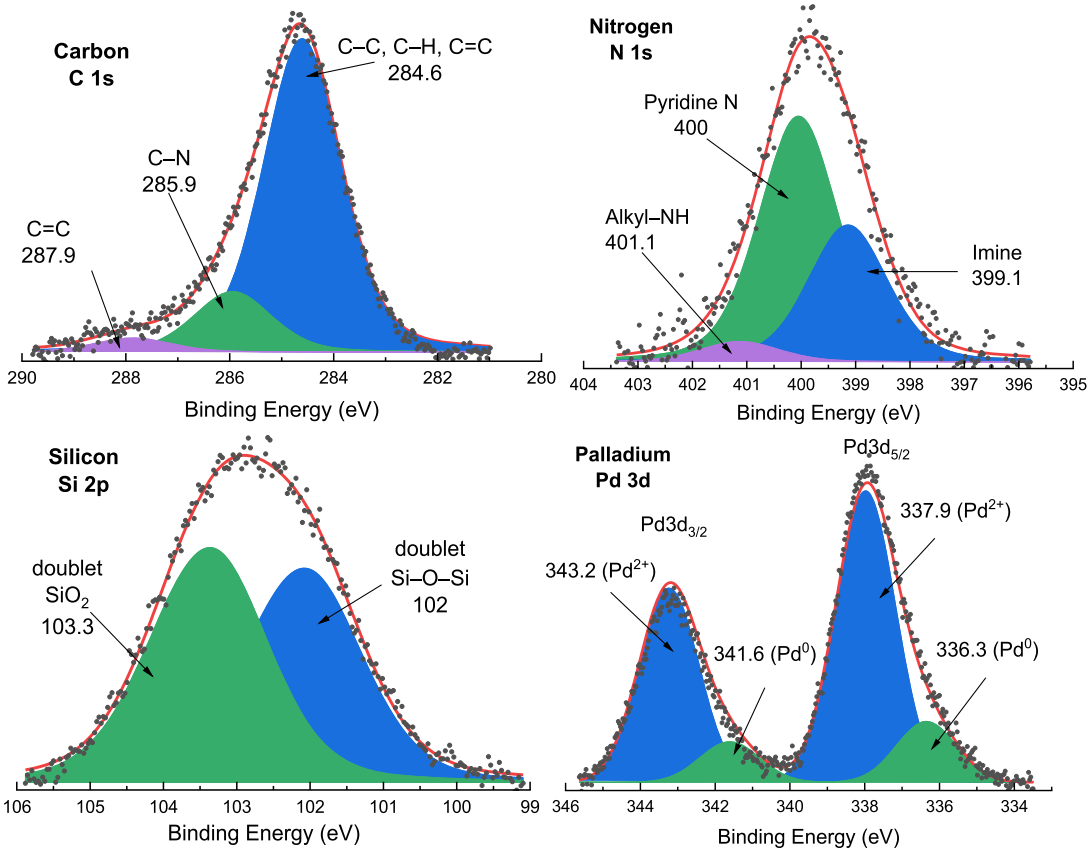

Figure 4. High-resolution XPS spectra of [PdL]–APTES–SiO_2 NPs. The measured datapoints are shown, the fitted individual peak contributions are highlighted in color, while the total fit is given by the red solid line.

coordination, the N 1*s* spectrum can be deconvoluted into three peaks; the binding energy of pyridine N (400 eV) and imine N (399.1 eV) is shifted to lower values by 1.1 and 0.5 eV. The third contribution at 401.1 eV is assigned to alkyl–NH. The S 2*p* peak was located at 163.5 eV and shifted slightly to a lower binding energy (162.8 eV) by 0.7 eV on metal coordination (Figure S19).[60,62] The Si 2*p* spectra of both materials (Figure 3 and 4) are deconvoluted into two doublets, centered around 103 eV for SiO_2 and 102 eV for Si–O–Si.[63] The Pd 3*d* core-level spectrum (Figure 4) exhibits the characteristic spin–orbit doublet consisting of the Pd $3d_{5/2}$ and Pd $3d_{3/2}$ components. Each component appears nonsymmetric, as they represent contributions of two oxidation states. For the $3d_{5/2}$, these are located at 336.3 and 337.9 eV and the corresponding ones for $d_{3/2}$ are found at 341.6 and 343.2 eV. These binding energies agree with the expected values of Pd(II) (343.2 and 337.9) and Pd(0) (341.6 and 336.3 eV). Similar binding energies have been reported for Pd(II) complexes of dithiocarbamates and poly(styryl)phenanthroline.[64,65] The binding energy for Pd(0) oxidation states is comparable with that of metallic Pd.[66–68]

2.5. Suzuki–Miyaura-Type C—C Coupling Catalysis

The [PdL]–APTES–SiO_2 precatalyst was investigated for the Suzuki–Miyaura cross-coupling reaction. In a first set of experiments, bromophenyl and phenylboronic acid were selected to find the optimum conditions (**Table 1**).

EtOH showed the best results out of the three tested solvents THF, EtOH, and H_2O, while K_2CO_3 showed the best results among the tested bases K_2CO_3, Na_2CO_3, and Et_3N (Table 1). Increasing the catalyst load from 0.4 to 0.6 and to 0.8 g increased the product formation. The same is true for increasing the reaction temperature from 60 to 80 °C, while increasing the temperature further to 100 °C did not give a higher yield. Reaction in water failed to yield the product, in line with a report on the N^N^S-coordinated cationic complex $[Pd(TSC\text{-}1)Cl]^+$ containing a 8-hydroxyquinoline-2-carbaldehyde TSC ligand which gave only 7% yield for the coupling of iodobenzene with phenylboronic acid in H_2O as solvent.[31] This stands in contrast to a report in which water-soluble sulfonized TSC Pd complexes such as the O^N^S coordinated [Pd(TSC-S)(PPh_3)] containing a 4-SO_3-salicylaldehyde-TSC ligand performed well with 92% yield for the standard Ph–Ph coupling in aqueous solution.[36]

We chose the optimized reaction conditions (Table 1), EtOH, K_2CO_3, at 80 °C for 20 h for coupling of further substrates (**Table 2**). Compared with the standard reaction between bromophenyl and phenylboronic acid, the yields of other substrates are slightly lower, which is due to the formation of undesired homocoupling products, which were removed. Bromobenzenes with electron-donating (CH_3, NH_2) groups show slightly higher yields compared to 4-dibromobenzene or

Research Article
doi.org/10.1002/ejic.202500245

Chemistry Europe
European Chemical Societies Publishing

Table 1. Results of Suzuki–Miyaura coupling reactions between bromobenzene and phenylboronic acid.

Entry[a)]	Solvent	Base	Catalyst load [g]	Temp. [°C]	Isolated yield [%]
1	THF	K_2CO_3	0.4	80	54
2	EtOH	K_2CO_3	0.4	80	70
3	H_2O	K_2CO_3	0.4	80	traces
4	EtOH	Na_2CO_3	0.4	80	50
5	EtOH	Et_3N	0.4	80	45
6	EtOH	K_2CO_3	0.6	80	75
7	EtOH	K_2CO_3	0.8	80	82
8	EtOH	K_2CO_3	0.8	60	66
9	EtOH	K_2CO_3	0.8	100	81

[a)]Reaction conditions: 146 mg (1.2 mmol) phenylboronic acid, 157 g (1 mmol) bromobenzene, 6 mmol base, 15 mL degassed solvent, 20 h reaction time. The optimum conditions are marked in gray. The biphenyl product was analyzed using ^{1}H NMR and ^{13}C-DEPTQ-[^{1}H] NMR spectroscopy, as well as GC–MS–HR–EI mass spectrometry (Figure S24–S26).

bromopyridines. 4-Pyridylboronic acid was successfully coupled to 1,4-dibromobenzene.

For the previously reported homogeneous S^N^O coordinated Pd(II) TSC precatalyst [Pd(TSC-2)(PPh_3)] containing a 3-acetyl-4-hydroxycoumarin-based TSC ligand (Scheme 1C), a yield of 78% for the coupling of iodobenzene with phenylboronic acid using EtOH, K_2CO_3, 1 mol% catalyst, 90 °C, in 6 h was reported.[31] A 97% yield was reported when using PEG-400 as solvent. Similar high yields were also reported for benzene derivatives containing electron-donating 4-Me and 4-MeO, while introduction of electron-withdrawing groups 4-NO_2 and 4-OHC gave slightly lower yields of around 87% in PEG-400.[31] The N^N^S-coordinated cationic complex [Pd(TSC-1)Cl]$^+$ containing a 8-hydroxyquinoline-2-carbaldehyde TSC ligand performed overall quite similar but showed only 71% yield in EtOH, K_2CO_3, 1 mol% catalyst, 90 °C, in 7 h and only 7% in H_2O as solvent. Thus, our catalyst system can easily compete with those from this report and also with that of other Pd(II) TSC catalyst systems, where maximum conversions ranging between 70% and 100% along with isolated yields ranging from 60% to 95% were reported.[31–42]

The very recently reported SiO_2-supported Pd(II) catalysts [Pd(NHC)Br_2(Py)] with the *N*-heterocyclic (NHC) ligand presumably bound to SiO_2 through an (benzimidazol-ylidene) *N*–ethyl–N(*i*Pr)–O–Si function showed 100% yield for the standard Ph–Ph coupling when using H_2O/*i*PrOH, K_2CO_3, 40 mg catalyst, at ambient temperature in 10 min,[14] while a Fe_3O_4@SiO_2 core–shell nanoparticle-supported Pd(NHC) complex based on benzimidazol-ylidene gave 92% yield under the otherwise same conditions, at 80 °C in 5 min.[17]

Recovery and washing of the [PdL]–APTES–SiO_2 precatalyst allowed recycling experiments. Using the standard conditions,

Table 2. Suzuki–Miyaura cross-coupling reaction of different aryl halides with phenylboronic acids.

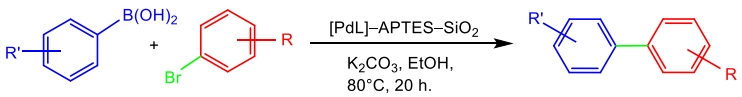

Substrate I[a)]	Substrate II	Product	Isolated yield [%]
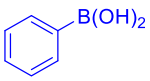	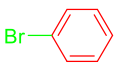		82
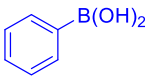	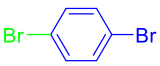	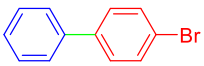	70
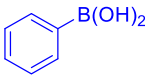	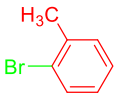	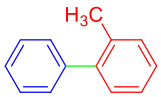	77
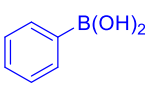	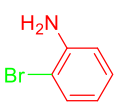	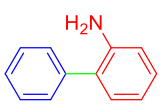	75
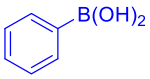	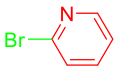		73
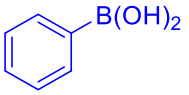	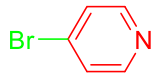	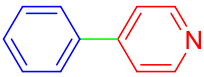	66
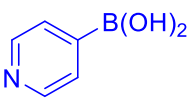	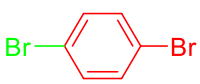	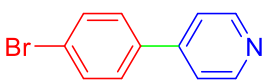	70

[a)]Reaction condition: 15 mL degassed solvent, 0.8 g catalyst, 6 mmol K_2CO_3, 1 mmol aryl-halide, 1.2 mmol aryl-boronic-acid, 80 °C, 20 h reaction time. The products were analyzed using ^{1}H NMR and ^{13}C-DEPTQ-[^{1}H] NMR spectroscopy, as well as GC–MS–HR–EI mass spectrometry (Figure S24–S44).

Research Article
doi.org/10.1002/ejic.202500245

Chemistry Europe
European Chemical Societies Publishing

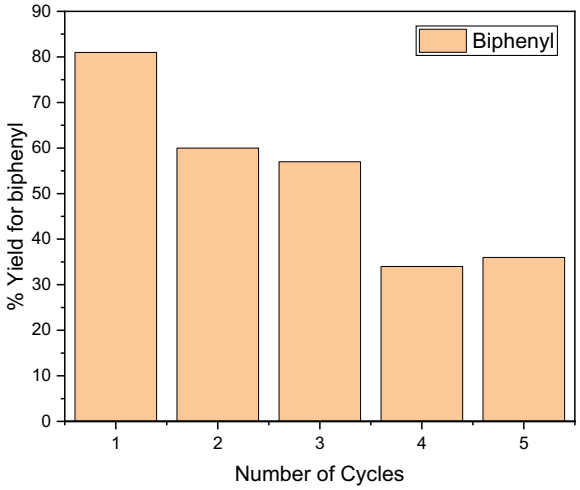

Figure 5. Recyclability of the [PdL]–APTES–SiO_2 catalyst for Suzuki–Miyaura coupling of biphenyl from bromobenzene and phenylboronic acid. The number of cycles refers to the recycled catalyst. Cycle No. 0 using the freshly prepared precatalyst gave 82% isolated yield.

0.8 g catalyst and K_2CO_3 as base in EtOH, 80 °C and a reaction time of 20 h with bromophenyl and phenylboronic acid as substrates, the yields dropped from the initial 82% to 80% for the first, to about 60% for the second and third cycle, and to about 35% for cycles 4 and 5 (**Figure 5**).

For the abovementioned homogeneous precatalyst [Pd(TSC-S)(PPh_3)] containing a 4-SO_3-salicylaldehyde-TSC ligand, the yields dropped from 93% to under 20% within 4 cycles.[34] The authors ruled out the formation of Pd particles from decoordination in the Pd(0) oxidation state during catalysis through addition of Hg.[34] At the same time, an Fe_2O_3-supported [Pd(NHC)Cl_2(*i*Pr)] precatalyst system providing a covalent imidazolydene-N–APTES–Fe_2O_3 conjugation showed high cycling stability for the coupling of 2-Me-iodobenzene and phenylboronic acid in DMF, $NaCO_3$, 50 °C, 12 h with a drop from 95% conversion (yield 87%) for the first cycle to 93% for the fifth cycle.[69]

In NMR-based stability experiments exposing the catalyst to EtOH solutions containing huge amounts of bromobenzene and phenylboronic acid, no changes in the NMR signatures of the two substrates were found, which would indicate reactions with Pd leached from the catalyst. In future experiments, various possibilities of catalyst deactivation, such as leaching of Pd(II) from the precatalyst material or leaching of Pd(0) from the reduced catalyst system through decoordination, will be studied through Pd-scavenging. Furthermore, the potential cleavage of covalent bonds of the conjugate under the catalytic conditions, which are in a far more dilute concentration regime than our preliminary NMR-based stability tests, will be investigated.

3. Conclusions

In the quest for a NP-supported palladium catalyst for the Suzuki–Miyaura cross-coupling reaction, three new TSCs based on 2,6-diacetyl-pyridine were synthesized. The parent bis(*N*4-(2-ethylphenyl)) 2,6-diacetyl-pyridine is potentially a pentadentate S^N^N^N^S ligand. Its 4-Cl-pyridine derivative allowed the covalent anchoring of the TSC onto monodispersed SiO_2 through reaction with APTES (3-aminopropyl)triethoxysilane) and subsequently coordination with Pd(II) through reaction with K_2PdCl_4. An H_2L–APTES conjugate was synthesized for comparison. The synthesis processes were monitored through FT-IR and UV–vis absorption spectroscopy. XPS of the thus produced [PdL]–APTES–SiO_2 conjugate particles of about 200 nm diameter (TEM) showed shifts in binding energies for the C—N and C═N groups of the TSC in both C 1s and N 1s spectra compared with the noncoordinated H_2L–APTES–SiO_2 conjugate. Cl atoms were not found which is in line with a tetradentate $S_{thiolate}$^$N1_{imine}$^$N_{Pyridine}$^$N2'_{amide}$ Pd(II) binding that was found for the model complex [Pd(L)] through single-crystal X-ray diffraction. The herein reported procedure of conjugating a TSC Pd(II) complex onto a SiO_2 NP support, thus, represents a robust and reliably method. The [PdL]–APTES–SiO_2 precatalyst showed potential in the Suzuki–Miyarua cross-coupling reaction, achieving up to 82% isolated yield. A recycling test showed a drop from initially 82% (cycle 0) to 80% after the first recycling of the catalyst. But then the isolated yields dropped to about 60% for cycles 2 and 3 and to about 35% for cycles 4 and 5. Compared with other homogeneous Pd(TSC) catalysts, this is a remarkable cycling stability; however, the peculiar two-cycle stepwise loss of activity must be studied in more detail focusing on potential catalyst deactivation pathways such as loss of Pd(0) from the reduced catalyst. Comparison with other catalytic Pd TSC systems also showed that our choice of EtOH, THF, and H_2O as solvent is very preliminary and other solvent might boost the performance of our catalytic system.

4. Experimental Section

Instrumentation

Powder X-ray diffractograms were recorded on an STOE-STADI MP diffractometer (STOE & Cie, Darmstadt, Germany) equipped with a Cu $K_{\alpha1}$ radiation ($\lambda = 0.15406$ Å) source and operating in transmission mode. Single-crystal X-ray structure determination of [Pd(L)] and the thiosemicarbazide *N*-(2-ethylphenyl)hydrazinecarbothioamide was carried out on a Bruker D8 Venture diffractometer (Bruker, Rheinhausen, Germany), including a Bruker Photon 100 CMOS detector, at 100(2) K using Mo Kα ($\lambda = 0.71073$ Å) radiation. The crystal data were collected using APEX4 v2021.10-0.[70] The structures were solved by dual-space methods using SHELXT, and the refinement was carried out with SHELXL employing the full-matrix least-squares methods on $F_O^2 < 2\sigma(F_O^2)$ as implemented in ShelXle.[71–73] The nonhydrogen atoms were refined with anisotropic displacement parameters, and hydrogen atoms were included using appropriate riding models. Data of the structure solutions and refinements can be obtained for *N*-(2-ethylphenyl)hydrazinecarbothioamide (CCDC 2218493) and the complex [Pd(L)] (CCDC 2248575) free of charge at https://summary.ccdc.cam.ac.uk/structure-summary-form or from the Cambridge Crystallographic Data Centre, 12 Union Road, Cambridge, CB2 1EZ, UK (fax: +44-1223336033 or e-mail: deposit@ccdc.cam.ac.uk). Selected crystallographic data and bond metrics are provided in Table S1 and S2, Supporting Information.

NMR spectra were recorded on a Bruker Avance II 300 MHz spectrometer (Bruker, Rheinhausen, Germany), using a triple resonance ^{1}H, nBB inverse probe head or a Bruker Avance III spectrometer at 499 MHz

Research Article
doi.org/10.1002/ejic.202500245

with a TCI prodigy 5 mm probe head (Varian, Troisdorf, Germany) with z-gradient ($^{1}H/^{19}F$, ^{13}C, ^{15}N, ^{2}H). HR-GC-EI/MS was recorded on a Thermo Scientific Exactive GC Orbitrap GC–MS system instrument (TriPlus RSH Autosampler, TRACE 1300 Series GC, Exactive GC-Orbitrap MS, Thermo Fisher Scientific, Darmstadt, Germany). HR-ESI-MS(+) spectra in positive mode were measured on a Thermo Scientific LTQ OrbitrapXL mass spectrometer with electron spray ionization and an FTMS Analyzer. FT-IR spectra were recorded on a PerkinElmer Spectrum 400 (Perkin Elmer, Waltham, MA, USA) with a Universal ATR sampling accessory in the range 4000 to 400 cm^{-1}. UV–vis absorption spectra were recorded using a Varian 60 Scan spectrophotometer. TGA of the materials was measured on a Perkin Elmer STA 6000 in the temperature range between 30 and 900 °C and scan rate of 10.0 °C min^{-1} under an N_2 atmosphere. Cyclic voltammetry was performed at a 100 mV s^{-1} scan rate in 0.1 M nBu_4NPF_6 solutions using a three-electrode configuration (working electrode: glassy carbon; counter electrode: Pt; reference: Ag/AgCl and a Metrohm Autolab PG STAT 30 potentiostat (Metrohm, Filderstadt, Germany) with ferrocene/ferrocenium as internal reference. TEM images were collected using Zeiss LEO912 (Zeiss, Oberkochen, Germany) at 120 kV accelerating voltage.

XPS was carried out in an ultrahigh vacuum system (base pressure 1×10^{-9} mbar). Samples for the XPS measurements were prepared by fixing a thin layer of the powder on a conductive copper tape, which was then transferred into the ultrahigh vacuum system. A non-monochromatic X-ray source (VG) with Mg-Kα excitation was used, having a photon energy of 1253.6 eV. The emitted photoelectrons were measured using a Specs Phoibos 100 hemispherical analyzer (Specs, Berlin, Germany). The powder samples exhibited slight charging effects during the measurement, which manifested as a uniform shift of all XPS signals toward higher binding energies by several electron volts. To account for this in the data analysis, the binding energy of the adventitious carbon peak was set to 284.7 eV, and the positions of all other peaks were adjusted accordingly. The XPS data were fitted by Voight profiles using the software "XPSPEAK 4.1" (http://xpspeak.software.informer.com/4.1/).

Computational studies were performed using ORCA 5.0.2[74,75]; def2-TZVP basis sets were used for all atoms.[76] The geometry of all compounds was optimized at the BP86 level of theory, using Grimme's Dispersion correction and the conductor-like polarizable continuum model (CPCM) parametrized for CH_2Cl_2 and dimethyl sulfoxide (DMSO) as an approximate solvation model.[77–81] The geometry optimization results were followed up with numerical frequency calculations to confirm the optimized structure's energetic minimum nature, as indicated by the absence of imaginary modes. Single-point and TD-DFT calculations were performed on the optimized geometries using the TPSSh functional, Grimme's D3 dispersion correction, and CPCM parametrized for CH_2Cl_2 and DMSO.[82] Chemcraft software was used for visualization of DFT calculation results.[83]

Syntheses: Materials

K_2PdCl_4 (98%) was supplied by Alfa Aesar, Germany (Thermofisher, Haverhill, MA, USA). $AgNO_3$ (99.5%) and CS_2 (99.9%) were purchased from Thermofisher, Germany (Thermofisher, Waltham, MA, USA); 2-ethylaniline (98%), hydrazine monohydrate (97%), 4-chloropyridine hydrochloride (99%), $(NH_4)_2S_2O_8$ (98%), 3-aminopropyl)triethoxysilane (APTES) (99%), bromobenzene (99%), and 2-bromoaniline (98%) were received from Sigma–Aldrich (Merck, Darmstadt, Germany). Pyruvic acid (96%), phenylboronic acid (98%), 4-pyridylboronic acid (98%), 1,4-dibromobenzene (98%), 2,6-diacetylpyridine (97%), pyridine-4-boronic acid (98%), 4-bromopyridine hydrochloride (95%), and 2-bromopyridine (98%) were purchased from BLDPharm Germany (BLDPharm, Cincinnati, OH, USA). The materials were used without further purification.

Syntheses: Synthesis of the 4-(2-Ethylphenyl)-Thiosemicarbazide

1.28 g (10.6 mmol) 2-ethylaniline was dissolved in 5 mL deionized water, and the temperature was brought to 0 °C. Thereafter, ice-cold CS_2 (16.4 mmol, 0.99 mL) was added to the solution, followed by adding 5 mL cold aqueous KOH (11.58 mmol, 0.649 g) solution. The solution was left for 24 h in an ice bath and refluxed for 2 h (80 °C) until 2-ethylaniline was completely consumed. A solution of hydrazine monohydrate (14 mmol, 0.7 mL) was added, and the reaction mixture was heated under reflux for 2.5 h. On cooling, a white precipitate formed. The precipitate was filtered off and washed with cold water and Et_2O. Recrystallization from MeOH/CH_2Cl_2 led to the isolation of white crystalline material. Single crystals were obtained from a solution of ethyl acetate (EtOAc) and cyclo-hexane (cHex) in a 1:1 ratio. Yield: 1.87 g (9.58 mmol, 90%). Elemental analysis for ($C_9H_{13}N_3S$, 195.08 g mol^{-1}): found (calculated) C 56.01 (55.35), H 6.80 (6.71), N 21.20 (21.52), S 16.24 (16.42). ^1H NMR (300 MHz, $CDCl_3$): $\delta = 9.04$ (s, 1 H), 8.22 (s, 1H), 7.61 (s, 1H), 7.28 (dd, $J = 5.9$, 2.6Hz, 3H), 4.03 (s, 2H), 2.67 (q, $J = 7.6$ Hz, 2H), 1.25 (t, $J = 7.6$ Hz, 3H) (NMR spectrum: Figure S1, Supporting Information). HR-GC-EI/MS: $[C_9H_{13}N_3S]^+$, Retention time = 22.90 min, >90% (Figure S7).

Syntheses: Synthesis of 4-Chloro-2,6-Diacetyl-Pyridine

4-Chloro-2,6-diacetyl-pyridine was synthesized modifying reported procedures.[84,85] Briefly, 2.3 g (1.58 mmol) 4-chloropyridine hydrochloride was dissolved in 5 mL deionized water and the pH was set to 9 using saturated NaOH solution. The mixture was extracted twice with 90 mL Et_2O, the combined organic fractions were dried over anhydrous Na_2SO_4, and the solvent was evaporated in a vacuum to obtain 4-chloropyridine as yellow oil. The freshly obtained 4-chloropyridine was poured into 100 mL H_2SO_4 (0.4 M), and then pyruvic acid (2.1 mL, 31.3 mmol), $AgNO_3$ (0.15 g, 0.9 mmol, suspended in 1 mL water), and $(NH_4)_2S_2O_8$ (11 g, 43.8 mmol) were added. The reaction mixture was stirred overnight at RT. The resulting solution was extracted with 2×150 mL CH_2Cl_2. The combined organic phases were washed with 5 mL water and subsequently dried over anhydrous Na_2SO_4. The crude product was obtained through evaporation of the solvent and purified using column chromatography (SiO_2, neat CH_2Cl_2). 4-Chloro-2,6-diacetyl-pyridine elutes first. Yield: colorless solid, 690 mg (3.49 mmol, 23%). Elemental analysis for ($C_9H_8NO_2Cl$, 197.62 g mol^{-1}), found (calculated): C 54.74 (54.70), H 4.04 (4.08), N 7.04 (7.09). ^1H NMR (300 MHz, $CDCl_3$): $\delta = 8.16$ (s, 2H), 2.75 (s, 6H) (Figure S2).

Syntheses of 2,6-Diacetyl-Pyridine-bis-(4-*N*-2-Ethylaniline)-Thiosemicarbazone (H_2L)

HL (1 mmol, 0.195 g) and 2,6-diacetyl-pyridine (0.333 mmol, 0.054 g) were dissolved in 10 mL AcOH. Then CF_3COOH (0.1 mL) was added and sonicated for 3 h at 40 °C. The yellow precipitate obtained was filtered and washed with water, saturated Na_2CO_3 and Et_2O. Yield: 70 mg (0.135 mmol, 49%). Elemental analysis for ($C_{27}H_{31}N_7S_2$, 517.21 g mol^{-1}): found (calculated): C 60.46 (62.64), H 6.24 (6.04), N 18.17 (18.94), S 12.72 (12.39). ^1H NMR (500 MHz, DMSO-d_6): $\delta = 10.67$ (s, 2H), 10.10 (s, 2H), 8.58 (d, $J = 7.9$ Hz, 2H), 7.79 (q, $J = 7.7$ Hz, 1H), 7.28 (dtt, $J = 11.7$, 5.9, 2.4Hz, 8H), 2.61 (q, $J = 7.6$ Hz, 4H), 2.54 (s, 6H), 1.22–1.04 (m, 6H). ^1H NMR (500 MHz, $CDCl_3$): $\delta = 9.20$ (s, 2H), 9.06 (s, 2H), 8.11–7.88 (m, 2H), 7.81–7.70 (m, 2H), 7.37–7.24 (m, 6H), 2.72 (q, $J = 7.6$ Hz, 4H), 2.55 (s, 6H), 1.28 (t, $J = 7.6$ Hz, 6H) (Figure S3). HR-ESI-MS(+) [*m/z*] = 518.21551 ($[H_2L + H^+]^+$, calc. 518.21551), 540.19732 ($[H_2L + Na]^+$, calc. 540.19745) (Figure S8).

Research Article
doi.org/10.1002/ejic.202500245

Syntheses of 4-Chloro-2,6-Diacetyl-Pyridine-Bis-(4-*N*-2-Ethylaniline)-Thiosemicarbazone (H_2L–Cl)

0.195 g (1 mmol) 4-(2-ethylphenyl)-thiosemicarbazide and 0.066 g (0.333 mmol) 4-chloro-2,6-diacetyl-pyridine were dissolved in 10 mL AcOH. Then, 0.1 mL CF_3COOH was added and the mixture was sonicated for 3 h at 40 °C. A yellow precipitate was obtained, filtered off, and washed with Et_2O. Yield: 160 mg (0.289 mmol, 29%). Elemental analysis for ($C_{27}H_{30}ClN_7S_2$, 552.16 g mol^{-1}): found (calculated): C 58.74 (58.73), H 5.47 (5.48), N 17.70 (17.76), S 10.61 (11.61). ^{1}H NMR (500 MHz, DMSO-d_6): $\delta = 10.67$ (s, 2 H), 10.20 (s, 2H), 8.72 (s, 2H), 7.37–7.21 (m, 8H), 2.61 (q, $J = 7.6$ Hz, 4H), 2.52 (s, 6H), 1.17 (t, $J = 7.6$ Hz, 6H). ^{1}H NMR (500 MHz, $CDCl_3$): $\delta = 9.34$–9.14 (m, 2H), 9.00 (d, $J = 22.7$ Hz, 2H), 7.98 (s, 2H), 7.88–7.70 (m, 2H), 7.37–7.27 (m, 6H), 2.71 (dd, $J = 15.0$, 7.5 Hz, 4H), 2.52 (s, 6H), 1.29 (dt, $J = 10.8$, 7.6 Hz, 6H) (Figure S4). HR-ESI-MS(+) [*m/z*] = 552.17690 ([H_2LCl + H^+]$^+$, calc. 552.17653), 574.15889 ([H_2LCl + Na]$^+$, calc. 574.15848) (Figure S9).

Syntheses of H_2L–APTES

0.12 g (0.22 mmol) H_2L–Cl was dissolved in THF (20 mL), and Et_3N (30 µL) was added. After 10 min, 52 µL (49 mg, 0.22 mmol) APTES ($M_W = 221.37$ g mol^{-1}, $\sigma = 0.946$ g mL^{-1}) was added. The mixture was stirred at RT for 4d. Then the solid was filtered off and dried. Yield: yellow powder 100.1 mg (736.34 g mol^{-1}, 73.78 mmol, 63%). ^{1}H NMR (300 MHz, $CDCl_3$): $\delta = 9.19$ (s, 2H), 8.92 (s, 2H), 7.98 (s, 2H), 7.87–7.78 (m, 2H), 7.36–7.27 (m, 6H), 5.66 (s, 1 H), 3.87–3.77 (m, 2H), 3.64 (q, $J = 7.3$ Hz, 2H), 2.73 (q, $J = 7.6$ Hz, 4H), 2.52 (s, 6H), 1.58 (s, 9H), 1.48 (t, $J = 7.3$ Hz, 6 H), 1.31 (t, $J = 7.6$ Hz, 6 H), 1.27–1.18 (m, 2H) (Figure S5). HR-ESI-MS(+) [*m/z*] = 737.344 ([H_2L–APTES + H^+]$^+$, calc. 737.344) (Figure S10).

Synthesis of [Pd(L)]

0.05 g (0.1 mmol) of H_2L was dissolved in 10 mL THF and Et_3N (0.05 mmol, 7 µL) was added. 30 mg (0.09 mmol) K_2PdCl_4 dissolved in 0.5 mL water was added and the mixture stirred for 30 min. The red precipitate was filtered off, washed with cold THF, and air-dried. Brick red solid 45 mg (0.072 mmol, 75%). Elemental analysis for ($C_{27}H_{29}N_7S_2$, 624.13 g mol^{-1}): found (calculated): C 52.16 (52.13), H 4.70 (4.70), N 15.72 (15.76), S 10.28 (10.31). ^{1}H NMR (300 MHz, DMSO-d_6): $\delta = 10.66$ (s, 2H), 10.50 (s, 2H), 10.09 (s, 2H), 9.42 (s, 1H), 8.58 (d, $J = 7.9$ Hz, 1H), 8.36 (t, $J = 8.0$ Hz, 1H), 8.19 (dd, $J = 8.3$, 1.1 Hz, 1H), 8.04–7.89 (m, 2H), 7.78 (t, $J = 7.9$ Hz, 1H), 7.43–7.09 (m, 12H), 2.75–2.61 (m, 8H), 2.54 (s, 6H), 2.08 (s, 6H), 1.23–1.05 (m, 12H) (Figure S6). HR-ESI-MS(+) [*m/z*] = 622.1044 ([H^1L + H^+]$^+$, calc. 622.1043) (Figure S11).

Synthesis of the NPs: APTES–SiO_2

Monodispersed SiO_2[86] and SiO_2–APTES conjugate NPs[87] were synthesized as previously reported. Elemental analysis for (APTES–SiO_2): C 12.24, H 2.86, N 4.08.

Synthesis of the NPs: H_2L–APTES–SiO_2

0.2 g H_2L–Cl was dissolved in 20 mL dry THF, degassed for 2 min and 100 µL Et_3N was added to the solution. 0.5 g APTES–SiO_2 was sonicated in 20 mL THF and added to the mixture. The reaction mixture was stirred for 4d at RT. The resulting solid was filtered off and washed with 3 × 50 mL THF. The colorless product was oven-dried at 40 °C for 24 h. Elemental analysis: C 4.77, H 1.37, N 1.44, S 0.33.

Synthesis of the NPs: [PdL]–APTES–SiO_2

0.1 g H_2L–APTES–SiO_2 was dissolved in 50 mL water through sonicating for 1 h. 320 mg (1 mmol) K_2PdCl_4 suspended in 5 mL THF was added and the reaction mixture was stirred for 3 h at RT. The yellow product was collected by filtration and washed with 20 mL of water, 20 mL THF, and 20 mL acetone and dried in an oven (40 °C) for 24 h.

Suzuki-Coupling Type Catalysis

The coupling of phenylboronic acid and bromobenzene was used as model reaction. In a typical experiment, 15 mL THF was degassed for 5 min, and then K_2CO_3 (6 mmol, 0.55 g), bromobenzene (1 mmol, 106 µL), phenylboronic acid (1.2 mmol, 0.146 g), and 0.4 g of the catalyst [PdL]–APTES–SiO_2 were added. The reaction was heated under reflux at 80 °C for 20 h. The resulting reaction mixture was allowed to cool to room temperature, extracted twice using ethyl acetate (20 mL), and dried over anhydrous Na_2SO_4. The crude product was purified using column chromatography (eluent: CH_2Cl_2/MeOH) to calculate the isolated yield of the individual reactions.

Recycling and reuse of the catalyst were tested for reuse by recovering the spent catalyst in a centrifuge tube, washing twice with 20 mL of water to remove the base and with 20 mL THF to remove the unreacted substrate and then left to dry in the fume hood overnight. The recovered catalyst was used as described above.

Acknowledgements

The authors thank Dr. Silke Kremer and Dr. Jörg Neudörfl at the X-ray Structural Analysis Platform of the Department of Chemistry and Biochemistry, University of Cologne for single-crystal and powder X-ray diffraction measurement. The authors also acknowledge Prof. Dr. Mathias Schäfer at the Department of Chemistry and Biochemistry, University of Cologne, for mass spectrometry analysis.

Open Access funding enabled and organized by Projekt DEAL.

Conflict of Interest

The authors declare no conflict of interest.

Author Contributions

Axel Klein: proposed the project. **Axel Klein**, **Sanjay Mathur**, and **Klaus Meerholz**: supervised the project. **Eric Tobechukwu Anthony**: carried out most of the experiments. **Selina Olthof**: conducted and fitted the XPS. **Stefan Roitsch**: conducted the TEM studies. **Axel Klein** and **Sanjay Mathur**: wrote the draft manuscript. **Axel Klein**, **Selina Olthof**, and **Sanjay Mathur:** revised the final version. All authors agree with the submitted version of the manuscript.

Data Availability Statement

The data that support the findings of this study are available from the corresponding author upon reasonable request.

Keywords: covalent functionalization · palladium · silica nanoparticles · Suzuki–Miyaura cross-coupling · thiosemicarbazones

[1] D. A. Kader, M. K. Sidiq, S. G. Taher, D. M. Aziz, *J. Organomet. Chem.* **2025**, *1030*, 123569.
[2] C. Caso, K.-H. Altmann, *Chem.–Eur. J.* **2025**, *31*, e202402664.
[3] I. H. Hasan, R. M. Mhaibes, A. A. H. Kadhum, H. A. Al-Bahrani, A. T. A. Imeer, N. A. M. Al-Rashedi, G. Shu, *J. Organomet. Chem.* **2025**, *1024*, 123444.
[4] M. Farhang, A. R. Akbarzadeh, M. Rabbani, A. M. Ghadiri, *Polyhedron* **2022**, *227*, 116124.
[5] M. C. D'Alterio, E. Casals-Cruañas, N. V. Tzouras, G. Talarico, S. P. Nolan, A. Poater, *Chem.–Eur. J.* **2021**, *27*, 13481.
[6] A. K. King, A. Brar, G. Li, M. Findlater, *Organometallics* **2023**, *42*, 2353.
[7] C. Len, S. Bruniaux, F. Delbecq, V. S. Parmar, *Catalysts* **2017**, *7*, 146.
[8] A. Vice, N. Langer, B. Reinhart, O. Kedem, *Inorg. Chem.* **2023**, *62*, 21479.
[9] A. Del Zotto, D. Zuccaccia, *Catal. Sci. Technol.* **2017**, *7*, 3934.
[10] M. R. Penny, Z. X. Rao, R. Thavarajah, A. Ishaq, B. J. Bowles, S. T. Hilton, *React. Chem. Eng.* **2023**, *8*, 752.
[11] S. P. Patil, S. N. Jadhav, F. A. Inamdar, M. A. Ameen, C. V. Rode, A. S. Rajmane, A. S. Kumbhar, *Chem. Pap.* **2023**, *77*, 5555.
[12] P. Hu, M. Kazemi, *J. Coord. Chem.* **2024**, *77*, 1324.
[13] E. O. Pentsak, L. U. Dzhemileva, V. A. D'yakonov, R. R. Shaydullin, A. S. Galushko, K. S. Egorova, V. P. Ananikov, *J. Organomet. Chem.* **2022**, *965–966*, 122319.
[14] M. Akkoç, H. K. Koç, I. Özdemir, *J. Mol. Struct.* **2025**, *1325*, 141006.
[15] T. Chen, Y. Pang, S. H. Ali, L. Chen, Y. Li, X. Yan, B. Wang, *Mol. Catal.* **2024**, *558*, 114045.
[16] M. L. Rahman, M. S. Sarjadi, M. S. Akhter, J. J. Hannan, S. M. Sarkar, *Arab. J. Chem.* **2022**, *15*, 103983.
[17] M. Akkoç, N. Bugday, S. Altın, N. Kiraz, S. Yasar, I. Özdemir, *J. Organomet. Chem.* **2021**, *943*, 121823.
[18] D. Sengupta, M. K. Pandey, D. Mondal, L. Radhakrishna, M. S. Balakrishna, *Eur. J. Inorg. Chem.* **2018**, *2018*, 3374.
[19] A. R. Hajipour, M. K. Tarrari, S. Jajarmi, *Appl. Organomet. Chem.* **2018**, *32*, e4171.
[20] S. Paul, M. M. Islam, S. M. Islam, *RSC Adv.* **2015**, *5*, 42193.
[21] A. A. Aly, E. M. Abdallah, S. A. Ahmed, M. M. Rabee, S. Bräse, *Molecules* **2023**, *28*, 1808.
[22] A. M. S. Hossain, J. M. Méndez-Arriaga, S. Gómez-Ruiz, J. Xie, D. H. Gregory, T. Akitsu, A. B. Ibragimov, G. Sun, C. Xia, *Polyhedron* **2023**, *244*, 116576.
[23] G. L. Parrilha, R. G. dos Santos, H. Beraldo, *Coord. Chem. Rev.* **2022**, *458*, 214418.
[24] S. Priyarega, J. Haribabu, R. Karvembu, *Inorg. Chim. Acta* **2022**, *532*, 120742.
[25] I. D. Kostas, B. R. Steele, *Catalysts* **2020**, *10*, 1107.
[26] N. P. Prajapati, H. D. Patel, *Synth. Commun.* **2019**, *49*, 2767.
[27] N. Arefyeva, A. Sandleben, A. Krest, U. Baumann, M. Schäfer, M. Kempf, A. Klein, *Inorganics* **2018**, *6*, 51.
[28] J. Hohnsen, L. Ryci, D. Obretenova, S. Jouchaghani, A. Klein, *Molecules* **2024**, *29*, 3680.
[29] S. Argibay-Otero, A. Núñez, L. Muñoz, R. Carballo, C. Fernandes, A. Paulo, E. M. Vázquez-López, *Eur. J. Inorg. Chem.* **2024**, *27*, e202400131.
[30] A. Haseloer, L. M. Denkler, R. Jordan, M. Reimer, S. Olthof, I. Schmidt, K. Meerholz, G. Hörner, A. Klein, P. Ni, *Dalton. Trans.* **2021**, *50*, 4311.
[31] B. Bera, P. Jana, S. Mandal, S. Kundu, A. Das, K. Chattopadhyay, T. K. Mondal, *Dalton. Trans.* **2024**, *53*, 11914.
[32] A. Castiñeiras, I. García-Santos, *Molecules* **2024**, *29*, 3425.
[33] S. Nandhini, S. Dharani, C. Elamathi, F. Dallemer, R. Prabhakaran, *Appl. Organomet. Chem.* **2021**, *35*, e6436.
[34] K. Thapa, P. Paul, S. Bhattacharya, *Inorg. Chim. Acta* **2019**, *486*, 232.
[35] J. Baruah, R. Gogoi, N. Gogoi, G. A. Borah, *Trans. Met. Chem.* **2017**, *42*, 683.
[36] L. C. Matsinha, J. Mao, S. F. Mapolie, G. S. Smith, *Eur. J. Inorg. Chem.* **2015**, *2015*, 4088.
[37] P. Paul, R. J. Butcher, S. Bhattacharya, *Inorg. Chim. Acta* **2015**, *425*, 67.
[38] A.-C. Tenchiu, I.-K. Ventouri, G. Ntasi, D. Palles, G. Kokotos, D. Kovala-Demertzi, I. D. Kostas, *Inorg. Chim. Acta* **2015**, *435*, 142.
[39] H. Yan, P. Chellan, Tingyi Li, J. Mao, K. Chibale, G. S. Smith, *Tetrahedron Lett.* **2013**, *54*, 154.
[40] J. Dutta, S. Bhattacharya, *RSC Adv.* **2013**, *3*, 10707.
[41] D. Pandiarajan, R. Ramesh, Y. Liu, R. Suresh, *Inorg. Chem. Commun.* **2013**, *33*, 33.
[42] P. Paul, S. Datta, S. Halder, R. Acharyya, F. Basuli, R. J. Butcher, S.-M. Peng, G.-H. Lee, A. Castineiras, M. G. B. Drew, S. Bhattacharya, *J. Mol. Catal.* **2011**, *344*, 62.
[43] H. S. Adhikari, A. Garai, M. Thapa, R. Adhikari, P. N. Yadav, *J. Macromol. Sci. Part A* **2022**, *59*, 211.
[44] T. A. Nguyen, T. A. Nguyen, D. B. Tran, H. D. C. Le, Q. L. Nguyen, V. Pham, *ACS Omega* **2020**, *5*, 14481.
[45] M. Jahangiri, F. Kiani, H. Tahermansouri, A. Rajabalinezhad, *J. Mol. Liq.* **2015**, *212*, 219.
[46] R. K. Sharma, G. Sharma, S. Gulati, A. Pandey, *Anal. Methods* **2013**, *5*, 1414.
[47] E. T. Anthony, M. Wilhelm, A. Klein, *ACS Appl. Nano Mater.* **2025**, *8*, 5841,
[48] C. I. C. Crucho, *Appl. Mater. Today* **2024**, *38*, 102179.
[49] A. Guerrero-Martínez, J. Pérez-Juste, L. M. Liz-Marzán, *Adv. Mater.* **2010**, *22*, 1182.
[50] G.-D. Sun, G.-H. Zhang, K.-C. Chou, A.-P. Dong, *Ind. Eng. Chem. Res.* **2017**, *56*, 12362.
[51] W. Stöber, A. Fink, E. Bohn, *J. Colloid Interface Sci.* **1968**, *26*, 62.
[52] T. Gholami, M. Salavati-Niasari, M. Bazarganipour, E. Noori, *Superlattices Microstruct.* **2013**, *61*, 33.
[53] D. M. Wiles, B. A. Gingras, T. Suprunchuk, *Can. J. Chem.* **1967**, *45*, 469.
[54] R. Basri, M. Khalid, Z. Shafiq, M. S. Tahir, M. U. Khan, M. N. Tahir, M. M. Naseer, A. C. Braga, *ACS Omega* **2020**, *5*, 30176.
[55] N. Moorthy, P. C. J. Prabakar, S. Ramalingam, G. V. Pandian, P. Anbusrinivasan, *J. Phys. Chem. Solids* **2016**, *91*, 55.
[56] R. N. Singh, A. Kumar, R. K. Tiwari, P. Rawat, *Spectrochim. Acta Part A Mol. Biomol. Spectrosc.* **2013**, *112*, 182.
[57] J. R. Durig, R. Layton, D. W. Sink, R. R. Mitchell, *Spectrochim. Acta* **1965**, *21*, 1367.
[58] S. Xiao, P. Xu, Q. Peng, J. Chen, J. Huang, F. Wang, N. Noor, *Polymers* **2018**, *10*, 930.
[59] X. Yan, T. Xu, G. Chen, S. Yang, H. Liu, Q. Xue, *J. Phys. D. Appl. Phys.* **2004**, *37*, 907.
[60] C. Zhang, X. Li, Z. Jiang, Y. Zhang, T. Wen, M. Fang, X. Tan, A. Alsaedi, T. Hayat, X. Wang, *ACS Sustain. Chem. Eng.* **2018**, *6*, 15644.
[61] Q. H. Thi, P. Man, L. Huang, X. Chen, J. Zhao, T. H. Ly, *Small Sci.* **2023**, *3*, 2200099.
[62] Y. He, Z. Shan, T. Tan, Z. Chen, Y. Zhang, *Polymers* **2018**, *10*, 930.
[63] R. Huang, M. Tang, W. Kan, H. Xu, K. Wu, Z. Wang, H. Li, *J. Phys. D. Appl. Phys.* **2024**, *57*, 15102.
[64] J. J. Criado, I. Fernandez, B. Macias, J. M. Salas, M. Medarde, *Inorg. Chim. Acta* **1990**, *174*, 67.
[65] Z. Zhuangyu, H. Hongwen, K. Tsi-Yu, *React. Polym. Ion Exch. Sorbents* **1988**, *9*, 249.
[66] K. S. Kim, A. F. Gossmann, N. Winograd, *Anal. Chem.* **1974**, *46*, 197.
[67] D. Zemlyanov, B. Aszalos-Kiss, E. Kleimenov, D. Teschner, S. Zafeiratos, M. Hävecker, A. Knop-Gericke, R. Schlögl, H. Gabasch, W. Unterberger, K. Hayek, B. Klötzer, *Surf. Sci.* **2006**, *600*, 983.
[68] L. P. A. Guerrero-Ortega, E. Ramírez-Meneses, R. Cabrera-Sierra, L. M. Palacios-Romero, K. Philippot, C. R. Santiago-Ramírez, L. Lartundo-Rojas, A. Manzo-Robledo, *J. Mater. Sci.* **2019**, *54*, 13694.
[69] P. D. Stevens, G. Li, J. Fan, M. Yen, Y. Gao, *Chem. Commun.* **2005**, *2005*, 4435.
[70] APEX4-Software Suite for Crystallographic Programs Bruker, A. APEX4-Software Suite for Crystallographic Programs. Inc., Madison, WI, USA **2021**
[71] G. M. Sheldrick, *Acta Crystallogr. A.* **2008**, *64*, 112.
[72] G. M. Sheldrick, *Acta Crystallogr. Sect. C Struct. Chem.* **2015**, *71*, 3.
[73] C. B. Hübschle, G. M. Sheldrick, B. Dittrich, *J. Appl. Crystallogr.* **2011**, *44*, 1281.
[74] F. Neese, F. Wennmohs, U. Becker, C. Riplinger, *J. Chem. Phys.* **2020**, *152*, 224108.
[75] F. Neese, *Mol. Sci.* **2022**, *12*, e1606.
[76] F. Weigend, R. Ahlrichs, *Phys. Chem. Chem. Phys.* **2005**, *7*, 3297.
[77] S. Grimme, S. Ehrlich, L. Goerigk, *J. Comput. Chem.* **2011**, *32*, 1456.
[78] S. Grimme, J. Antony, S. Ehrlich, H. Krieg, *J. Chem. Phys.* **2010**, *132*, 154104.
[79] A. D. Becke, *Phys. Rev. A* **1988**, *38*, 3098.
[80] J. P. Perdew, W. Yue, *Phys. Rev. B* **1986**, *33*, 8800.
[81] V. Barone, M. Cossi, *J. Phys. Chem. A* **1998**, *102*, 1995.

[82] J. Tao, J. P. Perdew, V. N. Staroverov, G. E. Scuseria, *Phys. Rev. Lett.* **2003**, *91*, 146401.
[83] Chemcraft. Chemcraft - Graphical Software for Visualization of Quantum Chemistry Computations
[84] R. Zong, H. Zhou, R. P. Thummel, *J. Org. Chem.* **2008**, *73*, 4334.
[85] D. Lieb, I. Kenkell, J. L. Miljković, D. Moldenhauer, N. Weber, M. R. Filipović, F. Gröhn, I. Ivanović-Burmazović, *Inorg. Chem.* **2014**, *53*, 1009.
[86] S. C. Feifel, F. Lisdat, *J. Nanobiotechnol.* **2011**, *9*, 59.
[87] B. Francis, B. Neuhaus, M. L. P. Reddy, M. Epple, C. Janiak, *Eur. J. Inorg. Chem.* **2017**, *2017*, 3205.

Manuscript received: May 8, 2025
Revised manuscript received: June 10, 2025
Version of record online: June 27, 2025